Desalination and Water Treatment
www.deswater.com
16 (2010) 339–353
April
1944-3994/1944-3986 © 2010 Desalination Publications. All rights reserved
doi: 10.5004/dwt.2010.1078

Thermodynamic analysis of humidification dehumidification desalination cycles

G. Prakash Narayan[a], Mostafa H. Sharqawy[a], John H. Lienhard V[a,*], Syed M. Zubair[b]

[a]*Department of Mechanical Engineering, Massachusetts Institute of Technology, Cambridge, USA*
Tel. +1-617-253-3790; email:lienhard@mit.edu
[b]*Department of Mechanical Engineering, King Fahd University of Petroleum and Minerals, Dhahran, Saudi Arabia*

Received 14 November 2009; Accepted 7 December 2009

ABSTRACT

Humidification dehumidification desalination (HDH) is a promising technology for small-scale water production applications. There are several embodiments of this technology which have been investigated by researchers around the world. However, from a previous literature [1], we have found that no study carried out a detailed thermodynamic analysis in order to improve and/or optimize the system performance. In this paper, we analyze the thermodynamic performance of various HDH cycles by way of a theoretical cycle analysis. In addition, we propose novel high-performance variations on those cycles. These high-performance cycles include multi-extraction, multi-pressure and thermal vapor compression cycles. It is predicted that the systems based on these novel cycles will have gained-output ratio in excess of 5 and will outperform existing HDH systems.

Key words: Humidification; Dehumidification; Desalination; Cycle analysis; Solar energy; Cycle optimization

1. Introduction

Widely used thermal desalination technologies such as multi-stage flash (MSF) and multi-effect distillation (MED) are not suitable for small scale (1–100 m^3/day) applications. Reverse osmosis (RO) is suitable for these applications but it requires a continuous supply of electrical or mechanical energy. Many developing countries which suffer from water scarcity also lack in resources which can generate these sources of energy (fossil fuels). However, some of these countries have an abundance of solar energy. Solar photovolatics can be used to operate reverse osmosis units for small scale applications in these countries. But it may not be feasible due to the high cost of PV modules and maintenance of RO systems [2]. A much simpler option is to use solar energy as a source of thermal energy. This requires us to develop desalination technologies which can use this energy in an efficient way.

One such technology, which mimics nature's water (rain) cycle, is the humidification dehumidification (HDH) desalination cycle. This technology has received ongoing attention in recent years and a few researchers have investigated specific realizations of this technology. The simplest form of the HDH process is illustrated in Fig. 1. The process consists of three subsystems: (a) an air and/or the water heater, which can use the solar energy; (b) a humidifier or the evaporator; and (c) a dehumidifier or the condenser. The cycle illustrated in Fig. 1 is just one embodiment of the HDH technology. The various cycle configurations are classified as closed-water open-air (CWOA) and closed-air open-water (CAOW) cycles. A closed-water open-air cycle [3–5] is one in which the air is taken in, humidified, partially dehumidified and

*Corresponding author.

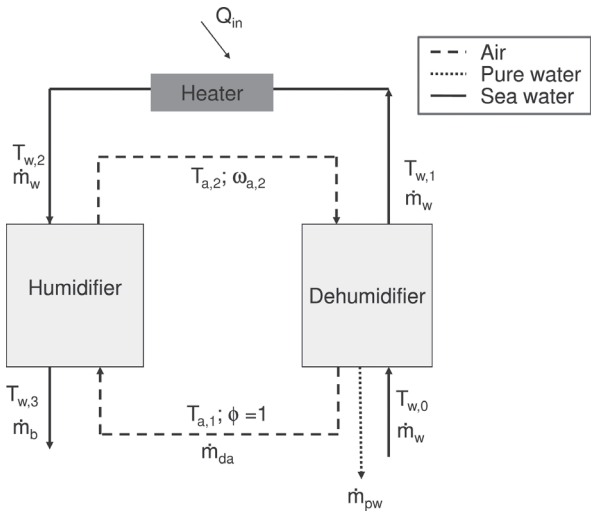

Fig. 1. Water-heated CAOW HDH cycle.

released in an open cycle while the water is recirculated, whereas in a closed air open-water cycle [6–9] the air is circulated in a closed loop between the humidifier and the dehumidifier while the water cycle is open loop. The air in these systems can be circulated by either natural convection or mechanical blowers. Also, these HDH systems are classified based on the type of heating used as water or air heating systems.

From the literature cited above and [1], we have found no study which systematically attempts to improve and/or optimize the cycle performance by modifying the cycle itself. Hence, the objective of this paper is to analyze the thermodynamic performance of various HDH cycles in literature and to propose novel high-performance variations on those cycles.

2. Modeling details

In order to evaluate the theoretical performance of various HDH cycles, a thermodynamic cycle analysis has been performed. In performing the analysis the following approximations have been made:

- The processes involved operate at steady-state conditions.
- There is no heat loss from the humidifier or the dehumidifier to the ambient.
- Pumping and blower power is negligible compared to the energy input to the heater.
- Kinetic and potential energy terms are neglected in the energy balance.
- The water condensed in the dehumidifier is assumed to leave at a temperature which is the average of the humid air temperatures at inlet and outlet of the dehumidifier.

The properties of moist air and liquid water are obtained from Engineering Equation Solver (EES) [10]. Dry air properties are evaluated using the ideal gas formulations presented by Lemmon [11]. Moist air properties are evaluated using the formulations presented by Hyland and Wexler [12], which are in close agreement with the data presented in ASHRAE Fundamentals [13]. EES calculates water properties using the IAPWS (International Association for Properties of Water and Steam) 1995 Formulation [14].

2.1. Governing equations

The equations governing a simple closed-air water-heated cycle are noted below. The nomenclature used is shown in Fig. 1.

Humidifier:

$$\dot{m}_w - \dot{m}_{da}(\omega_{a,2} - \omega_{a,1}) = \dot{m}_b \tag{1}$$

$$\dot{m}_b\, h_{w,3} - \dot{m}_w\, h_{w,2} = \dot{m}_{da}(h_{a,1} - h_{a,2}) \tag{2}$$

$$\dot{S}_{gen,h} = \dot{m}_b\, s_{w,3} - \dot{m}_w\, s_{w,2} + \dot{m}_{da}(s_{a,2} - s_{a,1}) \geq 0 \tag{3}$$

Dehumidifier:

$$\dot{m}_{pw} = \dot{m}_{da}(\omega_{a,2} - \omega_{a,1}) \tag{4}$$

$$\dot{m}_w(h_{w,1} - h_{w,0}) + \dot{m}_{pw}\, h_{pw} = \dot{m}_{da}(h_{a,2} - h_{a,1}) \tag{5}$$

$$\dot{S}_{gen,d} = \dot{m}_w(s_{w,1} - s_{w,0}) + \dot{m}_{da}(s_{a,1} - s_{a,2}) + \dot{m}_{pw}\, s_{pw} \geq 0 \tag{6}$$

Heater:

$$\dot{Q}_{in} = \dot{m}_w(h_{w2} - h_{w1}) \tag{7}$$

$$\dot{S}_{gen,ht} = \dot{m}_w(s_{w2} - s_{w1}) \geq 0 \tag{8}$$

These equations cannot be solved as there are two extra unknowns compared to the number of equations. Component effectivenesses are defined to close the set of equations.

2.2. Component effectiveness

An energy effectiveness (analogous to the effectiveness defined in heat exchanger design) is defined here. This definition is based on the maximum thermodynamic performance that can be achieved in an adiabatic heat and mass exchanger. Figure 2 illustrates the second law limitations imposed on a counterflow cooling tower. In the Figure, 'wb, 1' is the wet bulb point of the air at the inlet to the

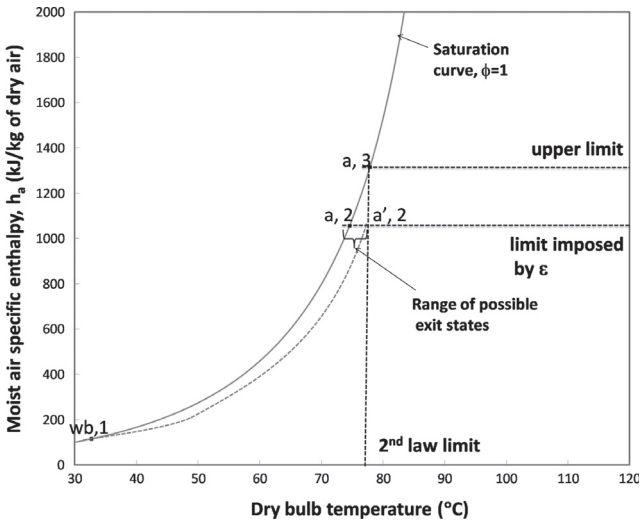

Fig. 2. Psychometric chart showing possible humidification paths and exit states; counter flow is assumed; $T_{wb,1} = 31.6°C$; $T_{a,3} = T_{w,2} = 77.9°C$.

humidifier and 'a, 2' is the exit air state. The air is assumed to be saturated at the inlet and hence, $T_{wb,1} = T_{a,1}$. The saturation line connecting the point 'wb, 1' to 'a, 2' represents one possible process path for the humidification process.

The maximum dry bulb temperature that can be achieved by the saturated air at the exit of the humidifier is the water inlet temperature (indicated by point 'a,3'). From Fig. 2, we see that the maximum enthalpy change possible ($\Delta\dot{H}_{max}$) for saturated air entering the humidifier occurs if the air can be brought to saturation at the water inlet temperature. The required energy is drawn from the water stream, which may or may not have the capacity rate ($\dot{m}_w c_{p,w}$) necessary to supply that amount of energy within the limits imposed by the air and water inlet temperatures. If the water stream lacks sufficient capacity, the maximum enthalpy change ($\Delta\dot{H}_{max}$) will be that which cools the water to the air inlet temperature. In this case the outlet air will be cooler than the water inlet temperature, and it may or may not be saturated.

Two parameters are required to fix the exit state of the air. In this analysis we fix the enthalpy and the relative humidity. The enthalpy is fixed indirectly by setting the effectiveness of the humidifier which is defined as the ratio of actual enthalpy change of either stream ($\Delta\dot{H}$) to maximum possible enthalpy change ($\Delta\dot{H}_{max}$).

$$\varepsilon = \frac{\Delta \dot{H}}{\Delta \dot{H}_{\max}} \tag{9}$$

In addition to defining the effectiveness, we need to fix the exit relative humidity to fully specify the cooling tower performance. For any given case, a particular range of exit relative humidities are possible (corresponding to points from 'a, 2' to 'a', 2' shown in Fig. 2). Hence, the relative humidity is treated as a variable in this study.

2.3. Solution technique

The equations were solved using the commercial software—EES which uses accurate equations to model the properties of moist air and water. EES is a numerical solver, and it uses an iterative procedure to solve the equations. The convergence of the numerical solution is checked by using the following two variables: (1) 'Relative equation residual'—the difference between left-hand and right-hand sides of an equation divided by the magnitude of the left-hand side of the equation; and (2) 'Change in variables'—the change in the value of the variables within an iteration. The calculations converge if the relative equation residuals are lesser than 10^{-6} or if change in variables is less than 10^{-9}. There are several publications which have previously used EES for thermodynamic analysis [15–18].

The code written in EES was checked for correctness against various limiting cases. For example, when $\varepsilon_h = \varepsilon_d = 0$ the Gained-output-ratio (GOR) was found to be 0 for all values of top and bottom temperatures. When $\varepsilon_h = 1$, the minimum stream-to-stream terminal (at exit or inlet) temperature difference in the humidifier was identically equal to zero for all values of top and bottom temperatures. Several other simple cases where checked. Also, calculations were repeated several times to check for reproducibility.

3. Performance and operating parameters

As a first step for understanding the HDH cycles the following performance parameters are defined.

1. *Gained-Output-Ratio (GOR):* is the ratio of the latent heat of evaporation of the water produced to the heat input to the cycle. This parameter is, essentially, the effectiveness of water production and an index of the amount of the heat recovery effected in the system.

$$\text{GOR} = \frac{\dot{m}_{pw}\, h_{fg}}{\dot{Q}_{in}} \tag{10}$$

   Latent heat is calculated with the operating pressure assumed as saturation pressure.
2. *Top temperature*: In HDH systems, either water or air is heated (for example, in a solar collector). The top temperature of the cycle is the temperature of the fluid being heated at the exit of the heater.

3. *Bottom temperature*: The feedwater to the dehumidifier enters the cycle at the bottom temperature of the cycle.
4. *Terminal temperature difference (TTD)*: is the stream-to-stream temperature difference at either end of the heat exchanger (humidifier /dehumidifier) [19].
5. *Pinch point temperature difference (P)*: is the minimum local stream-to-stream temperature difference at any point within the heat exchanger and is lower than both the terminal temperature differences [19]. In some cases, however, the pinch can be equal to one of the terminal temperature differences.
6. *Modified heat capacity ratio (HCR)*: For heat and mass exchange devices like the humidifier and the dehumidifier, we had previously [20] defined a parameter called the modified heat capacity ratio. The modified heat capacity ratio is the ratio of maximum possible enthalpy change of the cold stream to the maximum possible enthalpy change of the hot stream.

$$\mathrm{HCR} = \frac{\Delta \dot{H}_{\max,\mathrm{cold}}}{\Delta \dot{H}_{\max,\mathrm{hot}}} \tag{11}$$

We had also shown that [20] based on the value of HCR, the component irreversibilities can be minimized for a given value of effectiveness and fixed inlet conditions.

4. Basic cycles

In this section, various cycle configurations have been modeled and a parametric study was performed to understand the dependence of various parameters on the cycle. These configurations include CAOW water-heated, CWOA water-heated and CAOW air-heated cycles. The parameters studied include top and bottom temperatures of the cycle, mass flow rate of the air and water streams, the humidifier and dehumidifier effectivenesses and the operating pressure. The performance of the cycles depends on the mass flow rate ratio (ratio of mass flow rate of water at the inlet of the humidifier to the mass flow rate of dry air through the humidifier), rather than on individual mass flow rates. Hence, in this and all the succeeding sections the mass flow rate ratio is treated as a variable. This was also noted by other investigators [8,21,22].

4.1. CAOW with water heating

One of the most commonly studied HDH cycles is the closed-air open-water water-heated (CAOW) cycle.

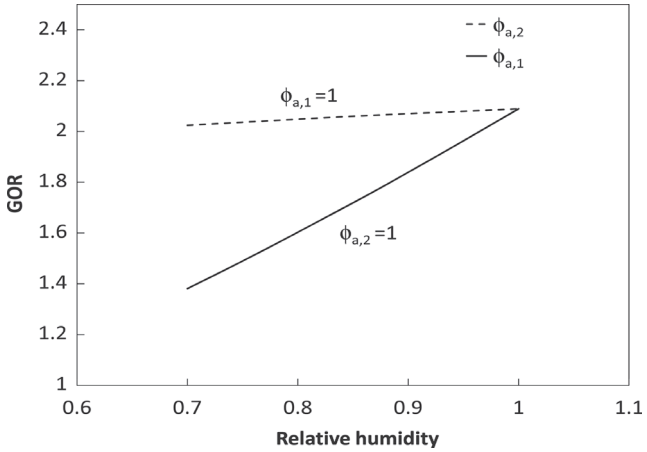

Fig. 3. Effect of humidifier and dehumidfier inlet air relative humidity on water-heated CAOW cycle performance. $\dot{m}_w$ = 0.5 kg/s; $\dot{m}_{da}$ = 0.1 kg/s; $T_{w,2}$ = 80°C; $T_{w,0}$ = 35°C; $\varepsilon_h = \varepsilon_d$ = 90%.

A comprehensive study of parameters which affect the performance of this cycle has not been reported in literature. Such a study will help to understand the ways by which the performance of this basic cycle can be improved and hence, is reported below.

Effect of relative humidity of the air entering and exiting the humidifier ($\phi_{a,1}$, $\phi_{a,2}$). The humidifier and dehumidifier can readily be designed such that the relative humidity of air at their exit is one. Hence, in this paper the exit air from these components is considered as saturated. However, the exit relative humidity is indicative of the performance of the humidifier and the dehumidifier and hence, understanding how a variation of these parameters change the performance of the system is important.

Figure 3 illustrates the effect that relative humidity of air at the humidifier inlet and exit can have on the performance of the cycle (GOR). For this particular case, the top ($T_{w,2}$) and bottom temperatures ($T_{w,0}$) were fixed at 80°C and 35°C respectively. Humidifier and dehumidifier effectivenesses (ε_h, ε_d) were fixed at 90%. Mass flow rate ratio was fixed at 5. It can be observed that for a variation of $\phi_{a,2}$ from 70 to 100% the performance of the system (GOR) reduces by roughly 3%, and for the same change in $\phi_{a,1}$ the effect is roughly 34%. This result suggest that the relative humidity of the air at the inlet of the humidifier has a much larger effect. These trends were found to be consistent for all values of mass flow rate ratios, temperatures and component effectivenesses. This, in turn, suggests that the dehumidifier performance will have a larger impact on the cycle performance. This issue is further investigated in the following paragraphs.

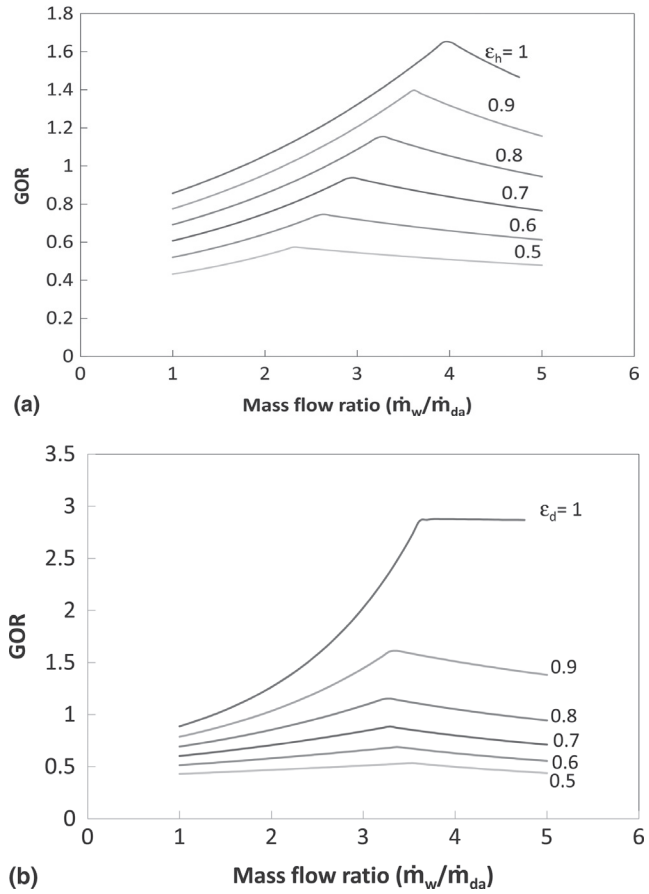

Fig. 4. Effect of component effectiveness on GOR for a water-heated CAOW cycle: (a) Effect of humidifier effectiveness. $T_{w,2}$ = 80°C; $T_{w,2}$ = 30°C; ε_d = 80%; (b) Effect of dehumidifier effectiveness. $T_{w,2}$ = 80°C; $T_{w,2}$ = 30°C; ε_h = 80%.

Effect of component effectiveness (ε_h, ε_d). Figure 4(a) and 4(b) illustrate the variation of performance of the cycle at various values of component effectivenesses. In Fig. 4(a), the top temperature is fixed at 80°C, the bottom temperature is fixed at 30°C and the dehumidifier effectiveness is fixed at 80%. The mass flow rate ratio was varied from 1 to 6. It is important to observe that there exists an optimal value of mass flow rate ratio at which the GOR peaks. It can also be observed that the increase in performance is fairly linear with increasing humidifier effectiveness, ε_h. In Fig. 4(b), the top temperature is fixed at 80°C, bottom temperature is fixed at 30°C, humidifier effectiveness is fixed at 80%. The cycle performance changes more dramatically for higher values of dehumidifier effectiveness. These trends are consistent for various values of top and bottom temperatures. Hence, a higher dehumidifier effectiveness is more valuable than a higher humidifier effectiveness for the performance (GOR) of the cycle.

In the previous discussion, we have observed that the dehumidifier exit air relative humidity ($\phi_{a,1}$) is more important than the humidifier exit air relative humidity ($\phi_{a,2}$). Hence, based on these results, we can say that for a water-heated cycle the performance of the dehumidifier is more important than the performance of the humidifier.

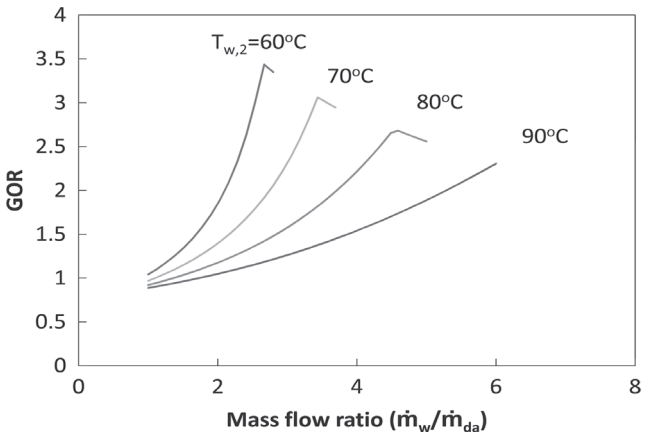

Fig. 5. Effect of top temperature, $T_{w,2,}$ on water-heated CAOW cycle performance. $T_{w,0}$ = 35°C; $\varepsilon_h = \varepsilon_d$ = 92%.

Effect of top temperature ($T_{w,2}$). Figure 5 illustrates the effect of top temperature on the cycle performance (GOR). In this particular case, the bottom temperature ($T_{w,0}$) was fixed at 35°C and humidifier and dehumidifier effectivenesses were fixed at 92%. Top temperature ($T_{w,2}$) was varied from 60°C to 90°C. The optimal value of mass flow rate ratio increases with an increase in top temperature. Depending on the humidifier and dehumidifier effectiveness this trend changes. At lower component effectivenesses, the top temperature has little or no effect on the cycle performance. This result is counter-intuitive. However, it can be explained using a new parameter called the modified heat capacity ratio. In [20], we had defined modified heat capacity ratio (HCR) as the ratio of maximum possible enthalpy change in the cold stream to the maximum possible enthalpy change in the hot stream. We had also described how the entropy generation in a heat and mass exchange device is minimized for a given effectiveness when HCR = 1 ('balanced' condition). We are going to use this understanding here to explain the trends obtained at various top temperatures.

Figures 6(a) and 6(b) show the variation of GOR with the heat capacity ratio of humidifier (HCR_h) and the dehumidifier (HCR_d) respectively. At the given inlet conditions the humidifier and dehumidifier are not balanced at the same point (same mass flow rate ratio). Hence the optimum GOR is not at HCR = 1 for both components. Rather, it can be seen that GOR maximizes at $HCR_h > 1$ and $HCR_d = 1$. The maximum occurs at a balanced condition for the dehumidifier which, as we have shown in the preceding paragraphs is the more important component.

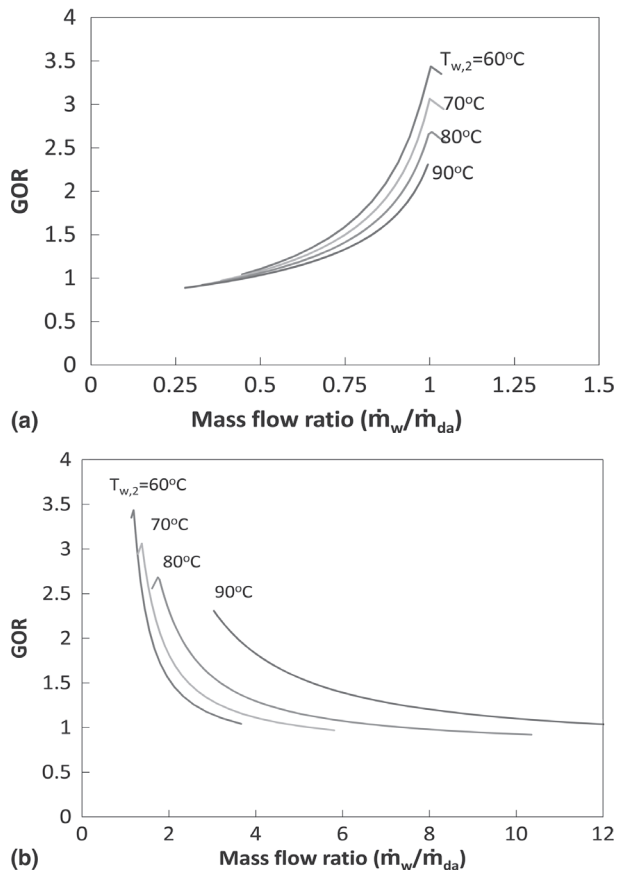

Fig. 6. Effect of top temperature plotted on GOR vs. HCR charts for a water-heated CAOW cycle. (a) GOR vs. HCR_d. $T_{w,0}$ = 35°C; $\varepsilon_h = \varepsilon_d = 92\%$; (b) GOR vs. HCR_h. $T_{w,0} = 35°C$; $\varepsilon_h = \varepsilon_d = 92\%$.

Further, it can be noticed that the degree of balancing of the humidifier at the optimum GOR condition reduces (HCRh moves farther away from 1) as the top temperature increases. Hence, the irreversibility of the humidifier (and the total irreversibility of the system) increases with increase in top temperature. A system with higher total irreversibility has a lower GOR [23]. This explains the decrease in GOR with top temperature. Also, as the top temperature increases the dehumidifier is balanced at higher mass flow ratio and hence the optimum value of GOR occurs at higher mass flow ratios.

Effect of bottom temperature ($T_{w,0}$). The bottom temperature of the cycle ($T_{w,0}$) is fixed by seawater temperature at the location where the water is drawn. Figure 7 illustrates a case with top temperature of 80°C and component effectivenesses of 92%. A higher bottom temperature of the cycle results in a higher value of GOR as illustrated in the figure. This result can again be understood by plotting HCR of humidifier and dehumidifier versus the GOR of the system (Fig. 8(a) and 8(b)). The degree of balancing of the humidifier at the optimum

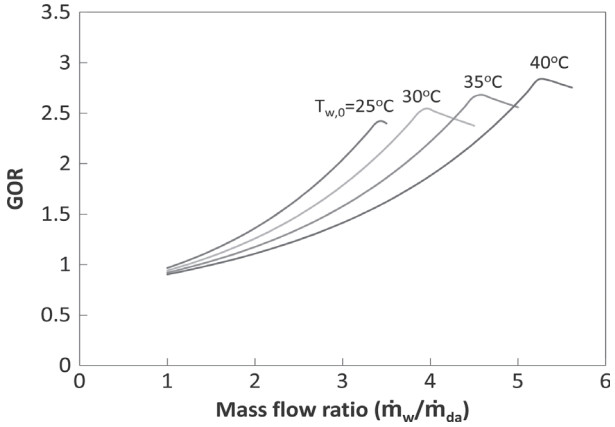

Fig. 7. Effect of bottom temperature, $T_{w,0}$, on water-heated CAOW cycle performance. $T_{w,2} = 80°C$; $\varepsilon_h = \varepsilon_d = 92\%$.

condition for GOR decreases with decrease in bottom temperature. Hence, the irreversibilities in the humidifier (and the total irreversibility of the system) increases with decreasing bottom temperature and GOR declines.

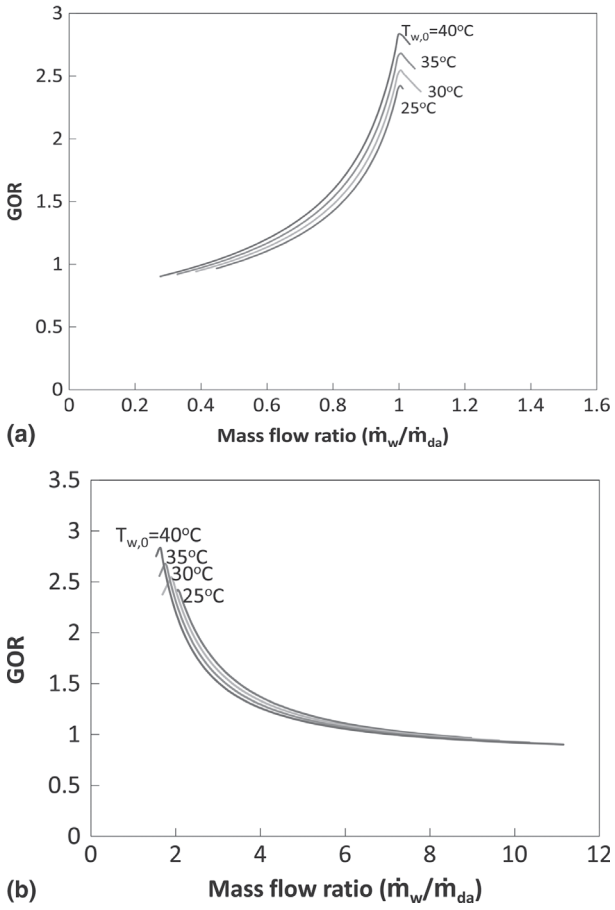

Fig. 8. Effect of bottom temperature plotted on GOR versus HCR charts for a water-heated CAOW cycle. (a) GOR vs. HCR_d. $T_{w,2} = 80°C$; $\varepsilon_h = \varepsilon_d = 92\%$; (b) GOR v HCR_h. $T_{w,2} = 80°C$; $\varepsilon_h = \varepsilon_d = 92\%$.

From the discussions in this subsection we have observed that the performance of the cycle (GOR) is a function of the following parameters.

$$\mathrm{GOR} = f(\mathrm{HCR}_h, \mathrm{HCR}_d, \varepsilon_h, \varepsilon_d, T_{w,2}, T_{w,0}, \phi_{a,2}, \phi_{a,1}) \quad (12)$$

The values of GOR reported in this paper for the CAOW water-heated cycle is within 20% of the experimental value obtained by Nawayseh et al. [9]. In section 5, we attempt to use the ideas developed thus far to improve the cycle performance.

4.2. CAOW with air heating

A simple air-heated cycle is one in which air is heated, humidified, and dehumidified [24–27]. Current simulations have found that the GOR for this cycle is very low (GOR < 1, only slightly better than a solar still). It is important to understand the reasons for this. The air in this cycle is heated and immediately sent to a humidifier where it is saturated. The air also gets cooled during the humidification process since it is at a higher temperature than the water stream. Thus, heat is lost to the water stream in the humidifier. In the water-heated cycle, the air stream is heated in the humidifier. This further facilitates heat recovery in the dehumidifier, which is absent in an air heated system. Hence, the performance is much lower in an air-heated system.

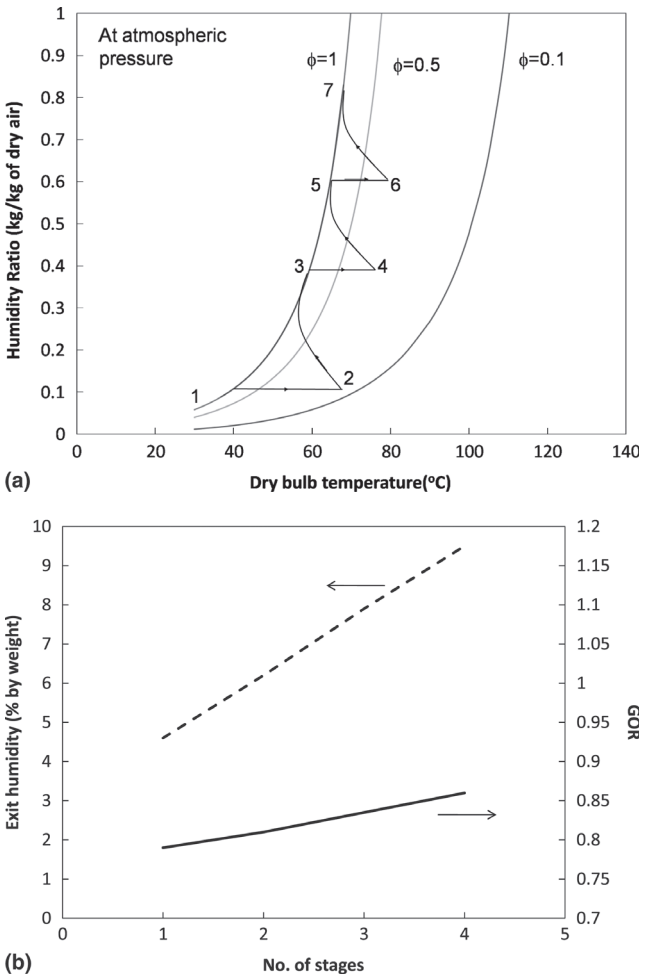

Fig. 9. Multi-stage CAOW air-heated cycle. (a) Representation in psychrometric coordinates; (b) Effect of number of stages on performance.

To improve the performance of air-heated systems, Chafik [24,28] proposed a multi-stage cycle. A three stage cycle is illustrated using a psychometric chart in Fig. 9(a). The air in this cycle is heated and sent to a humidifier where it is saturated. It is then further heated and humidified again. The idea behind this scheme was to increase the exit humidity of the air so that water production can be increased. Chafik was able to increase the exit humidity from 4.5% (by weight) for a single stage system to 9.3% for a 4 stage system. We reproduce this result for the same cycle under similar operating conditions. However, we also observed that the GOR of the cycle rises by only 9% (Fig. 9(b)). This is because the increased water production comes at the cost of increased energy input. This, in turn, is because the multi-staging does not improve the heat recovery in the humidification process. Chafik reported very high cost of water production of the range of 15–50 €/m^3 due in part to the large area of solar collectors required for this low GOR system.

4.3. CWOA with water heating

Another cycle commonly treated in the literature is the closed-water open-air (CWOA) water-heated cycle [3–5]. Because air is not saturated, as in a closed air cycle, the wet bulb temperature is much lower and hence the water in the humidifier can be cooled to a much lower temperature than in the closed air cycle. Thus, one might expect that the humidifier effectiveness will influence the cycle performance non-linearly, unlike in the closed air cycle.

Figure 10(a) shows the variation of cycle performance for various values of humidifier effectiveness. This figure is plotted for a top temperature of 80°C, bottom temperature of 30°C and $\varepsilon_d = 80\%$. For higher values of ε_h (90% and 100%), the second law of thermodynamics is violated and hence, the performance at those points are not plotted. Unlike in heat exchangers (with no phase change or mass transfer) where the second Law is not violated if $\varepsilon < 1$, the pinch point temperature difference

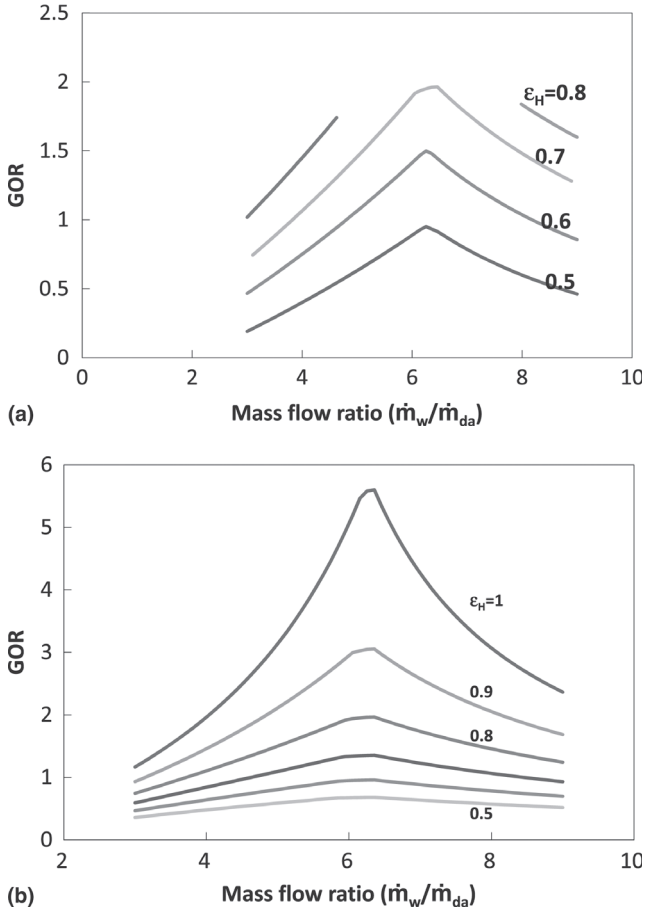

Fig. 10. Effect of component effectiveness on GOR for a CWOA water-heated cycle. (a) Effect of humidifier effectiveness. $T_{a,3} = 80°C$; $T_{a,1} = 35°C$; $\phi_{a,1} = 60\%$; $T_{w,0} = 30°C$; $\varepsilon_d = 80\%$; (b) Effect of dehumidifier effectiveness. $T_{a,3} = 80°C$; $T_{a,1} = 35°C$; $\phi_{a,1} = 60\%$; $T_{w,0} = 30°C$; $\varepsilon_h = 80\%$.

in the humidifier and the dehumidifier occurs at a position between the two ends of the heat exchanger. As a result even when $\varepsilon < 1$ (minimum terminal temperature difference $TTD_{min} > 0$) the second Law can be violated ($\dot{S}_{gen} < 0$) in the humidifier and the dehumidifier.

The variation of GOR with humidifier effectiveness is linear, unlike our expectation. Figure 10(b) confirms that the variation of performance of the cycle with dehumidifier effectiveness is non-linear, as in the closed air cycle. Hence, the thermodynamic design of this cycle is similar to that of a closed-air water heated cycle.

5. Improved cycles

Several important observations made in the previous section can be leveraged to modify the basic cycles in literature to improve the performance of these cycles. In this section, such an attempt is made and several novel cycles which have improved performance are identified.

5.1. High efficiency, air heated cycle

In the previous section we noted that the air heated cycle is inefficient. Yet, the air heated cycle is of practical significance as a solar air heater itself is expected to be more simple (and hence, more economical) than a solar water heater [29]. All the studies in literature consider cycles that heat the air before the humidifier (in single or multistage), which causes heat recovery to be reduced since the air is cooled in the humidifier. If the heater is placed after the humidifier, saturated air from the humidifier is heated and sent to the dehumidifier (Fig. 11(a)). An enthalpy-temperature diagram of the proposed cycle is shown in Fig. 11(b).

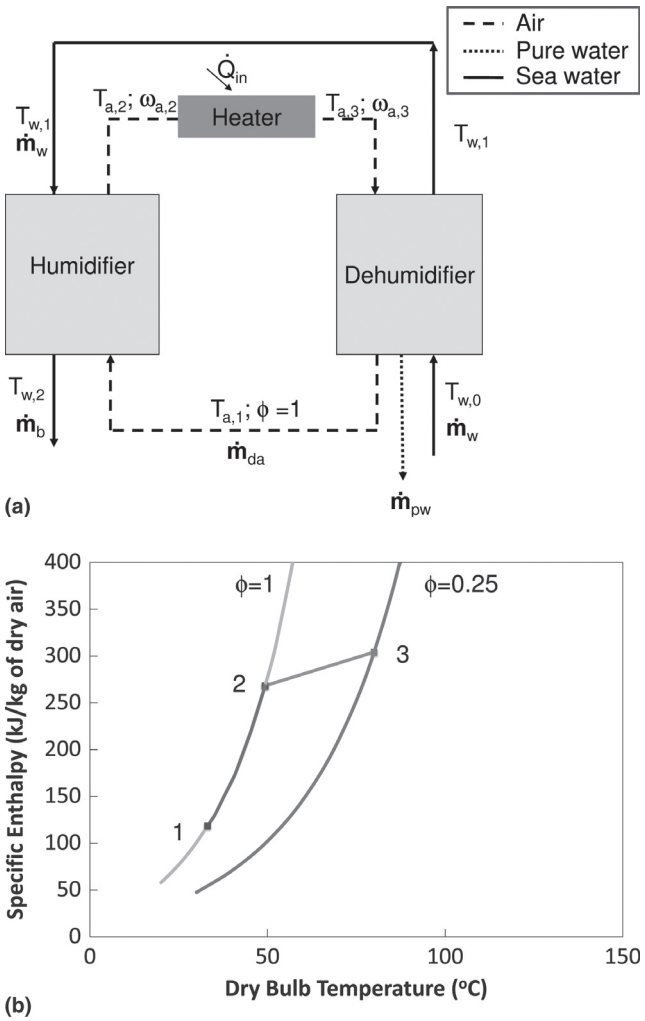

Fig. 11. Modified air-heated cycle. (a)Schematic diagram; (b) Psychometric representation: humidification (1-2) followed by heating (2-3) and subsequent dehumidification (3-1).

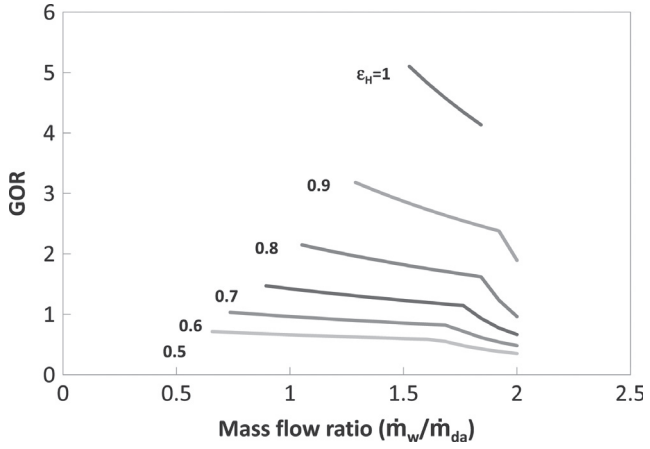

Fig. 12. Effect of humidifier effectiveness on CAOW modified air-heated cycle performance $T_{a,3} = 80°C$; $T_{w,0} = 30°C$; $\varepsilon_d = 90\%$.

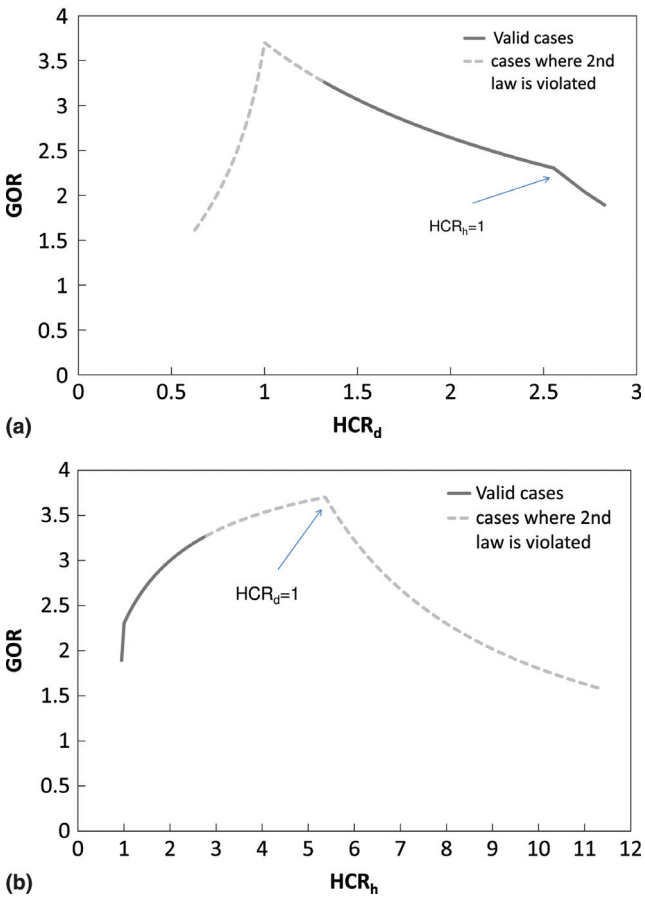

Fig. 13. Effect of heat capacity ratio on CAOW modified air-heated cycle performance. (a) Effect of HCR_d.$T_{a,3} = 80°C$; $T_{w,0} = 30°C$; $\varepsilon_h = \varepsilon_d = 90\%$; (b) Effect of HCR_h. $T_{a,3} = 80°C$; $T_{w,0} = 30°C$; $\varepsilon_h = \varepsilon_d = 90\%$.

This cycle has following advantages. It operates the air heater at a higher temperature level and it can be observed from the properties of moist air that at a higher temperature level it is easier to raise the temperature of saturated air than at a lower temperature level. So a given top temperature can be attained by a smaller heat input. Also, the heat is recovered in the humidifier since the water stream is heating the air stream (and humidifying it) in the humidifier. Hence, the overall heat recovery is much improved in this cycle. This cycle can be realized in two ways, closed air or closed water. We describe the closed air cycle below.

Figure 12 shows the performance of the proposed system. This figure is plotted for a top temperature of 80°C, bottom temperature of 30°C and $\varepsilon_d = 90\%$. As can be observed from the figure, the proposed cycle is several times more efficient (300%) than the air heated cycle. The performance of this system is higher than the water heated cycle (by 25%). From Fig. 12 we can also observe that the variation of performance with humidifier effectiveness is non-linear for the proposed cycle, unlike the water heated cycles. GOR is plotted only for those mass flow rate ratios in which the cycle satisfies second law requirements.

The performance curve of the cycle plotted in Fig. 12 can be better explained using the modified heat capacity ratio. Figures 13(a) and 13(b) show the variation of GOR with modified heat capacity ratio of dehumidifier and humidifier respectively. The global maximum in the GOR occurs at $HCR_d = 1$ and $HCR_h = 5.35$. There is a small kink in the curve at $HCR_h = 1$. The global maximum is not realized as second law is violated at that point. This is because for the given inlet conditions we are not able to completely balance the dehumidifier without violating the second law. Also, from these figures, it is important to note that the balancing of the dehumidifier is more important than the balancing of the humidifier to the modified air-heated cycle.

5.2. Multi-extraction air-heated cycle

The performance of the air-heated system can be increased if we are able to bring the HCR values of both of the components closer to one. This can be achieved by manipulating the mass flow rate of water or air. We choose to do so with air as it is easier to extract and re-circulate air without changing the components too much. More specifically, we extract air at various points from the humidifier and inject it at corresponding points in the dehumidifier (Fig. 14). The idea behind this is to breakup the humidifier and dehumidifier into a number of smaller parts with different values of mass flow rate ratio. Ideally, the mass flow rate ratio should be

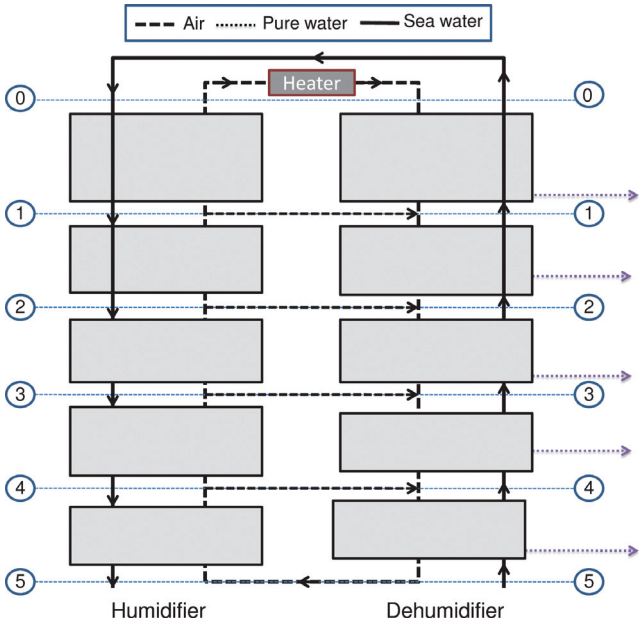

Fig. 14. Multi-extraction CAOW modified air-heated cycle.

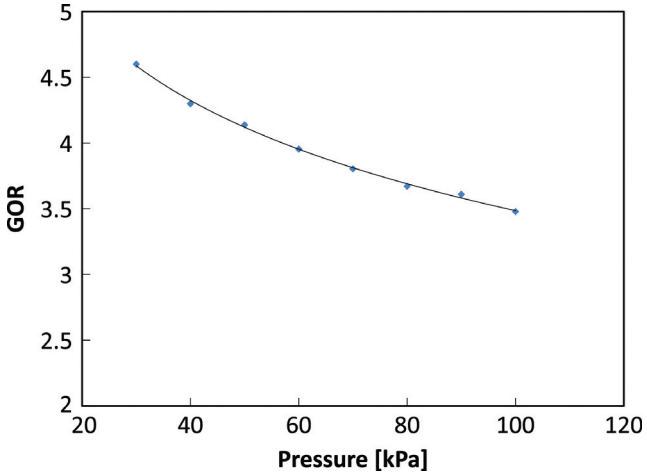

Fig. 15. Effect of system pressure on performance of CAOW modified air-heated cycle; $T_{a,3} = 67°C$; $T_{w,0} = 30°C$; $\varepsilon_h = \varepsilon_d = 90\%$.

selected such that each of these smaller parts should be operating very close to a HCR of 1 (so that the entropy production in the humidifier and the dehumidifier is minimized [20]). Müller-Holst [6] implemented a similar concept in his HDH system but with the objective of balancing stream-to-stream temperature difference. However, the minimum entropy generation is at a point where HCR = 1 which is not the same as the situation in which temperature differences are balanced.

The optimization has been performed by looking at inlet conditions to the humidifier and dehumidifier in various planes in the cycle diagram. These are represented as planes 0 to 5 in Fig. 14. It is not possible to attain balanced condition for the humidifier and the dehumidifier without changing the inlet conditions as we have observed in previous examples (Fig. 13(a), 13(b)). This is achieved by splitting the humidifier and dehumidifier into many parts such that each part has the required inlet conditions and required mass flow ratio to achieve the balanced condition. A detailed example of multi-extraction cycle is found in [20].

5.3. Sub-atmospheric pressure, air heated cycle

We had previously observed [1] that all the HDH systems in literature operate at atmospheric pressures only. The humidity ratios are much higher at pressures lower than atmospheric pressure. For example, at a dry bulb temperature of 60°C and a pressure of 50 kPa, the saturation humidity ratio is roughly 150% higher than at atmospheric pressure. Hence, it is logical to design an air heated cycle (section 5.1) to operate at sub-atmospheric pressures [30]. Figure 15 shows the variation of performance of this cycle with change in system pressure. This data is for a top temperature of 67°C, a bottom temperature of 35°C, $\varepsilon_h = 80\%$, $\varepsilon_d = 80\%$ and optimized values of mass flow rate ratio.

The GOR of the cycle at a pressure of 30 kPa is 4.5. This is a 30% increase in performance. However, we have observed that the performance increase comes at the expense of a lower humidifier TTD and a greater heat transfer area. Also, from the many designs we have examined for this cycle, we have observed that the exit humidity from the dehumidifier is higher than in the atmospheric pressure case. Hence, the cycle has a possible scope for further improvement.

5.4. Varied pressure cycle

To get better performance out of the HDH cycle, the exit humidity from the dehumidifier should be minimized. The novel cycles explained in the previous sub-sections can be combined to form a new cycle which will operate the humidification process under sub-atmospheric conditions and the dehumidification at a higher pressure than the humidification process. The energy for the cycle is input to the air stream after the humidification, in the form of air compression. The compressed air is then dehumidified. The air after dehumidification can be expanded to a lower pressure and a part of the compressor work may be then supplied by the expander. This will maximize exit humidity from humidifier and minimize exit humidity from dehumidifier. Figure 16(a) shows an illustration of this system [31]. This system will combine the benefits of

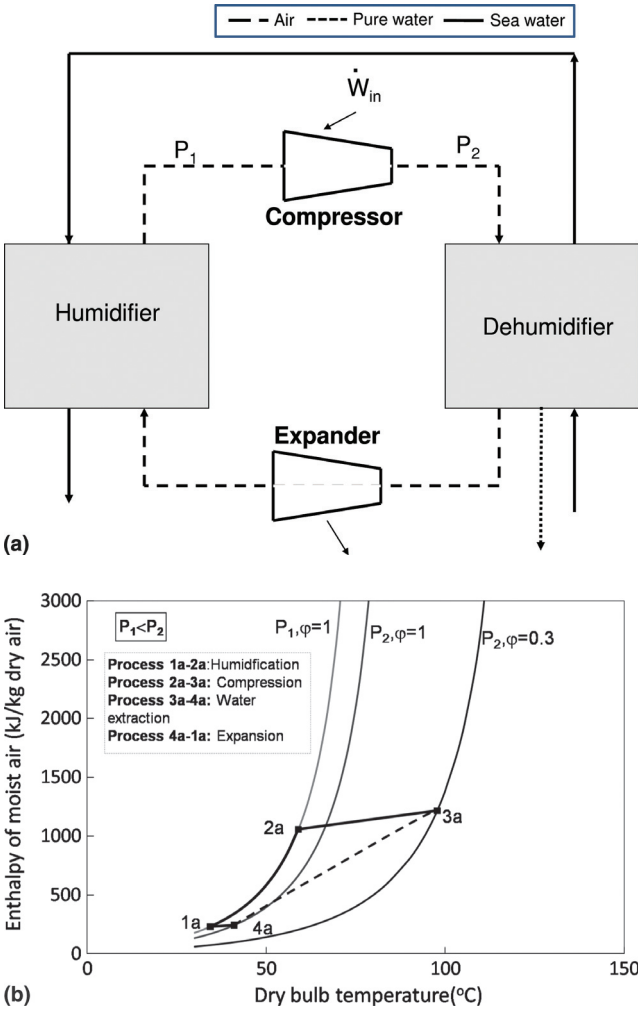

Fig. 16. Varied pressure cycle. (a) Schematic diagram; (b) Psychometric representation: humidification (1-2) followed by compression (2-3), subsequent dehumidification (3-4) and finally expansion (4-1).

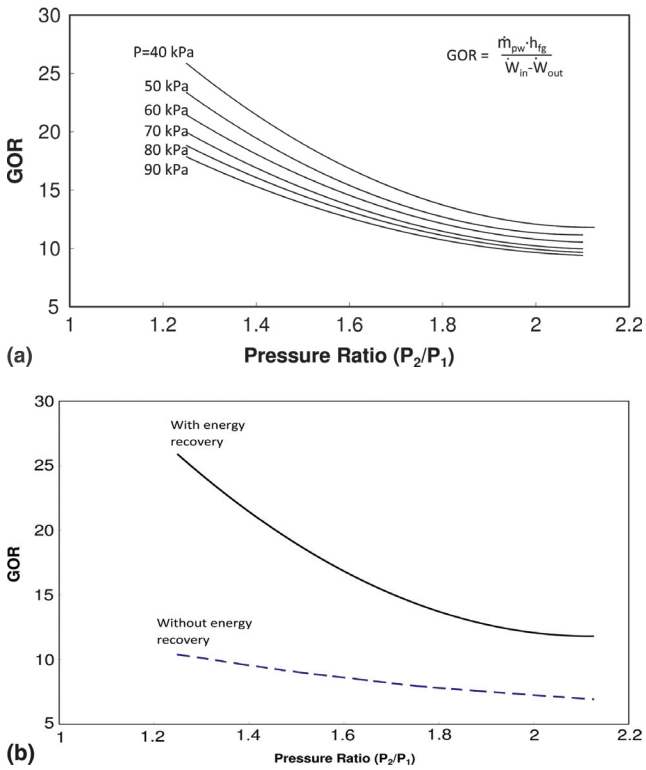

Fig. 17. Performance of a varied pressure cycle. (a) Effect of pressure ratio and humidifier pressure: $T_{w,0} = 30°C$; $\varepsilon_h = \varepsilon_d = 90\%$; $\eta_C = \eta_E = 90\%$; (b) Effect of work recovery: $T_{w,0} = 30°C$; $\varepsilon_h = \varepsilon_d = 90\%$; $\eta_C = \eta_E = 90\%$.

the systems discussed in sections 5.1 and 5.3. To quantify this, an analysis was carried out.

Figure 17(a) shows the effect of humidifier pressure and pressure ratio on the system performance. This graph is plotted for a bottom temperature of 30°C, $\varepsilon_h = 90\%$, $\varepsilon_d = 90\%$, $\eta_c = 90\%$ and $\eta_e = 90\%$. Here GOR is defined as the ratio of the product of mass flow of water produced and latent heat to the net work input to the system.

$$\mathrm{GOR} = \frac{\dot{m}_{pw}\, h_{fg}}{\dot{W}_{in}} \tag{13}$$

As expected, lower humidifier pressures give a higher performance. This is because the humidity ratios are higher at lower pressures. Moreover, at lower pressure ratios we have a higher performance. TTD becomes smaller at lower pressure ratios. Hence, the higher performance at lower pressure ratios is at the expense of a larger heat exchanger area.

We have explored the possibility of recovering part of the work as an expansion at the exit of the humidifier. This expansion cools the inlet air to the humidifier. The lower temperature to the humidifier improves the performance. Figure 17(b) shows the effect of work recovery for a two-pressure system operating at a humidifier pressure of 40 kPa. It can be seen that an efficient work recovery device will reduce the energy demand by upto 150%. An example of such a system with work recovery is also shown in the figure. This system has a GOR of 25 for reasonable values of TTD (5°C for the non-contact heat exchanger and 3°C for the packed bed). The higher GOR results in part from the use of mechanical work, rather than heat, as the cycle's energy source.

5.5. Thermal vapor compression in HDH

From the analysis in the previous section, we can observe that the pressure driven HDH system has

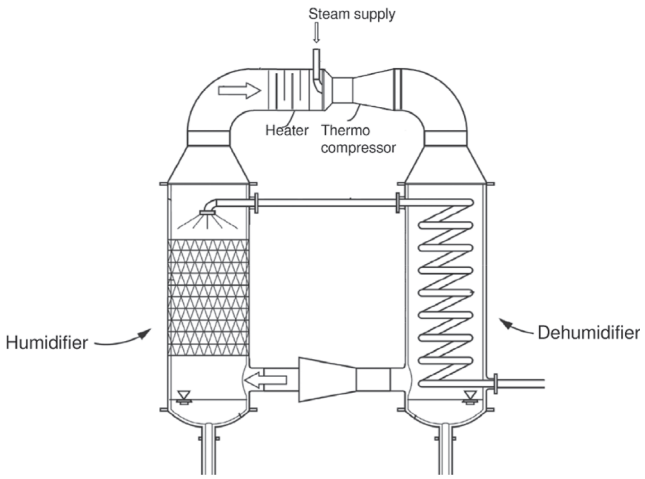

Fig. 18 Thermocompression driven HDH cycle.

very high performance comparable with conventional desalination systems. We should, however, keep in mind that these high values of GOR are based on mechanical or electrical energy input to the compressor. An alternative design of the varied pressure system uses a thermocompressor in place of the mechanical compressor. Figure 18 illustrates a possible configuration of this cycle in which an air heater and a steam ejector are used to provide energy to the varied pressure cycle. It was found that for a design of the steam ejector, the mass of steam required per unit mass of fresh water produced was about 0.1 and for every 100 kg of air circulated only about 6 kg of steam was required to operate the thermocompressor. This steam could be supplied from an associated power plant as is typical in other coproduction systems for water and electricity. A GOR of 5 is achieved for this case. GOR is defined, like in conventional HDH systems, as the ratio of the heat of evaporation of the distillate produced to the heat input to the system.

$$\mathrm{GOR} = \frac{\dot{m}_{pw}\, h_{fg}}{\dot{Q}_{in} + \dot{Q}_{steam}} \tag{14}$$

where, $\dot{Q}_{in}$ is the heat input in the heater and $\dot{Q}_{steam}$ is the heat of the steam entering the system.

$$\dot{Q}_{steam} = \dot{m}_{steam}\, h_{steam} \tag{15}$$

Further investigation into the design of this system is currently in progress. It should be noted that these systems are not thermally balanced. A balanced system would have a much higher performance value. It is possible to balance these systems using the concepts explained earlier [20].

Table 1
Comparison of HDH cycles.

CYCLE	GOR
CAOW Air heated cycle	0.78
CAOW Multi-stage Air heated cycle (four stage)	0.85
CAOW Water heated cycle	2.5
CWOA Water heated cycle	2.6
CAOW Modified air heating	3.5
CWOA Modified air heating	3.5
Reduced pressure cycle (35 kPa)	4.5
Multi-extraction air heated cycle	>4.5
Thermo-compression cycle	5
Varied pressure cycle (work driven)	25
Ideal (reversible) HDH cycle	122

6. Comparison of cycles

The various HDH cycles analyzed in this paper are compared in Table 1. The comparison is based on the gained-output-ratio. The bottom temperature for all the cycles is maintained at 35°C. The top temperature for all the cycles is maintained at 90°C. These cycles are designed for humidifier $\mathrm{TTD}_{\mathrm{min}}$ of > 2.8°C and dehumidifier $\mathrm{TTD}_{\mathrm{min}}$ of > 4°C. Using a simple thermodynamic analysis of a reversible system the maximum possible GOR was calculated as 122 (see appendix).

Some very important observations can be made from Table 1. The commonly used air-heated cycles are much less efficient than the water-heated cycles (GOR is roughly 2.5 times larger for the water-heated case). Multi-staging for air-heated cycles does not improve the performance greatly. However, the proposed modification to the air-heated cycle (section 5.1) can make it better than the water heated cycle (GOR is 25% larger than the water-heated cycle and >300% better than the common air-heated cycles).

Müller-Holst [6] quoted a high value of GOR (3 to 4.5) for a system which has balanced stream-to-stream temperature difference in the components. We also observed similar values of GOR using the concept of balancing. Balancing the components in a cycle for heat capacity ratio close to one improves the performance greatly. For a multi-extraction air heated cycle (explained in section 5.2), the GOR can reach a value of 4.5. Vacuum operation improves the performance of the air-heated cycle further, but at the expense of larger heat and mass transfer area. An air-heated HDH cycle which is balanced and is operating under sub-atmospheric conditions is a very efficient thermally-driven HDH system. Varied pressure HDH if driven by thermo-compression can be more efficient (GOR >5) than the air-heated system. Performance will depend on our ability to design an efficient ejector and also on the availability of steam.

7. Conclusions

A comprehensive study to understand and optimize the performance of HDH cycles has been carried out. The following significant conclusions are arrived at from this study:

1. The performance of a basic water-heated cycle depends on: (a) the modified heat capacity ratio in the humidifier and the dehumidifier; (b) the humidifier and dehumidifier effectivenesses; (c) top and bottom temperatures and (d) relative humidity of air at the exit of the humidifier and the dehumidifier.
2. The air-heated cycles previously reported in the literature are inefficient. A novel air-heated cycle has been proposed in this paper. This new cycle is more efficient than even the water-heated cycle.
3. Closed air and closed water cycles have similar thermodynamic characteristics and hence similar performance.
4. The dehumidifier is more vital than the humidifier to the performance of a conventional water-heated cycle. However, for the novel air-heated cycle proposed in this paper both the humidifier and dehumidifier effectivenesses have similar impact on the cycle performance.
5. Balancing the humidifier and the dehumidifier to attain HCR close to 1 will improve performance greatly. In all of the studied cycles, balancing the dehumidifier was found to yield a higher performance than balancing the humidifier.
6. The novel concept of operating HDH under vacuum is proposed in this paper. Vacuum operation increases performance but at the expense of heat exchanger size.
7. Varied pressure systems which have better performance than single pressure systems have also been proposed in this paper. These systems can be mechanically or thermally driven. They have high performance compared to all conventional HDH systems.

Acknowledgments

The authors would like to thank King Fahd University of Petroleum and Minerals for funding the research reported in this paper through the Center for Clean Water and Clean Energy at MIT and KFUPM.

Nomenclature

Symbols		*Units*
$\bar{g}$	specific molar Gibbs energy	J/mol
GOR	gained output ratio	-
h	specific enthalpy	J/kg
$\bar{h}$	specific molar enthalpy	J/mol
h_{fg}	latent heat of vaporization	J/kg
$\dot{H}$	total enthalpy rate	W
HCR	heat capacity ratio	-
$\dot{m}$	mass flow rate	kg/s
$\dot{n}$	molar flow rate	mol/s
P	absolute pressure	Pa
$\dot{Q}_{in}$	heat rate input	W
s	specific entropy	J/kg·K
$\bar{s}$	specific molar entropy	J/mol·K
$\dot{s}_{gen}$	entropy generated	W/K
T	temperature	°C
$\dot{W}_{in}$	work rate input	W

Greek Symbols

ω	absolute humidity of dry air	kg_w/kg_a
η	isentropic efficiency	-
ε	component effectiveness	-
ϕ	relative humidity	-

Subscripts

a	humid air
b	brine
c	compressor
d	dehumidifier
da	dry air
e	expander
h	humidifier
ht	heater
pw	pure water
w	seawater

References

[1] G.P. Narayan, M.H. Sharqawy, E.K. Summers, J.H. Lienhard V, S.M. Zubair and M.A. Antar, The potential of solar-driven humidification-dehumidification desalination for small-scale decentralized water production, Renewable and Sustainable Energy Reviews, 14(4) (2010), 1187–1201.
[2] D. Manolakos, E. Sh. Mohamed, I. Karagiannis, and G. Papadakisa, Technical and economic comparison between PV-RO system and RO-Solar Rankine system. Case study: Thirasia island, Desalination, 221 (2008) 37–46.
[3] Y.J. Dai and H.F. Zhang, Experimental investigation of a solar desalination unit with humidification and dehumidification, Desalination, 130 (2000) 169–175.
[4] M. Khedr, Techno-Economic Investigation of an Air Humidification-Dehumidification Desalination Process, Chemical Engineering Technology, 16 (1993) 270–274.

[5] G. Al-Enezi, H.M. Ettouney and N. Fawzi, Low temperature humidification dehumidification desalination process. Energy Conversion and Management, 47 (2006) 470–484.
[6] H. Müller-Holst, Solar Thermal Desalination using the Multiple Effect Humidification (MEH) method in Solar Desalination for the 21st Century, Springer, Dordrecht, 2007.
[7] J.F. Klausner, R. Mei and Y. Li, Innovative Fresh Water Production Process for Fossil Fuel Plants, U.S. DOE - Energy Information Administration annual report, 2003.
[8] S. Al-Hallaj, M.M. Farid and A.R. Tamimi, Solar desalination with humidification dehumidification cycle: performance of the unit, Desalination, 120 (1998) 273–280.
[9] N.K. Nawayseh, M.M. Farid, S. Al-Hallaj and A.R. Tamimi, Solar desalination based on humidification process-Part I. Evaluating the heat and mass transfer coefficients, Energy Conversion Management, 40 (1999) 1423–1439.
[10] S.A. Klein, Engineering Equation Solver. Academic Professional, Version 8. http://www.fchart.com/ees/ees.shtml
[11] E.W. Lemmon, R.T. Jacobsen, S.G. Penoncello and F. Daniel, Thermodynamic Properties of Air and Mixtures of Nitrogen, Argon, and Oxygen from 60 to 2000 K at Pressures to 2000 MPa, J. Physical and Chemical Reference Data, 29(3) (2000) 331.
[12] R.W. Hyland and A. Wexler, Formulations for the Thermodynamic Properties of the Saturated Phases of H_2O from 173.15 K to 473.15 K. ASHRAE Transactions Part 2Ã, Paper 2793, 1983.
[13] D.J. Wessel, ASHRAE Fundamentals Handbook 2001 (SI Edition), American Society of Heating, Refrigerating, and Air-Conditioning Engineers, 2001.
[14] A. Prufi and W. Wagner, The IAPWS formulation 1995 for the thermodynamic properties of ordinary water substance for general and scientific use, J. Physical and Chemical Reference Data, 31(2) (1995) 387–535.
[15] W. Pridasawas and P. Lundqvist, A year-round dynamic simulation of a solar driven ejector refrigeration system with isobutane as a refrigerant, International Journal of Refrigeration, 30(5) (2007) 840–850.
[16] R. Zmeureanu and X.Y. Wu, Energy and energy performance of residential heating systems with separate mechanical ventilation, Energy, 32(3) (2007) 187–195.
[17] B.A. Qureshi and S.M. Zubair, A complete model of wet cooling towers with fouling in fills, Applied Thermal Engineering, 26(16) (2006) 1982–1989.
[18] Z. Wei and R. Zmeureanu, Exergy analysis of variable air volume systems for an office building, Energy Conversion and Management, 50(2) (2009) 387–392.
[19] R.K. Shah and D.P. Sekulic, Fundamentals of heat exchanger design, Wiley, NY, 2003.
[20] G.P. Narayan, J.H. Lienhard V and S.M. Zubair, Entropy generation minimization in combined heat and mass exchange devices (Submitted for publication, 2009).
[21] S.M. Soufari, M. Zamen and M. Amidpour, Performance optimization of the humidification-dehumidification desalination process using mathematical programming, Desalination, 237 (2009) 305–317.
[22] M.M. Farid and A.W. Al-Hajaj, Solar desalination with humidification dehumidification cycle, Desalination, 106 (1996) 427–429.
[23] K.H. Mistry, J.H. Lienhard V and S.M. Zubair, Second Law Analysis of Humidification-Dehumidification Desalination Cycles (submitted for publication, 2009).
[24] E. Chafik, A new type of seawater desalination plants using solar energy, Desalination, 156 (2003) 333–348.
[25] I. Houcine, M.B. Amara, A. Guizani, and M. Maalej, Pilot plant testing of a new solar desalination process by a multiple-effect-humidification technique, Desalination, 196 (2006) 105–124.
[26] M. Ben-Amara, I. Houcine, A. Guizani and M. Maalej, Experimental study of a multiple-effect humidification solar desalination technique, Desalination, 170 (2004) 209–221.
[27] C. Yamali and I. Solmus, A solar desalination system using humidification dehumidification process: experimental study and comparison with the theoretical results, Desalination, 220 (2008) 538–551.
[28] E. Chafik, Design of plants for solar desalination using the multi-stage heating/humidifying technique, Desalination, 168 (2004) 55–71.
[29] J.A. Dufie and W.A. Beckmann, Solar energy thermal processes, Wiley, NY, 1974.
[30] M.H. Sharqawy, J.H. Lienhard V, G.P. Narayan and S.M. Zubair, Water separation under reduced pressure, US Patent application #12/554,726, 2009.
[31] G.P. Narayan, M.H. Sharqawy, J.H. Lienhard V and S.M. Zubair, Water separation under varied pressure, US Patent application #12/573,221, 2009.

Appendix

Calculation of Carnot GOR for HDH

The highest GOR achievable in a cycle of this type will be that for zero entropy production.

We derive here the expression for this upper limit. Figure 19 shows the application of the 1st and 2nd law to the system.

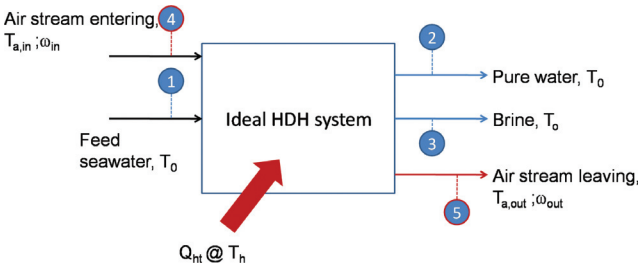

Fig. 19. Schematic diagram for calculating Carnot GOR of HDH.

$$\dot{Q}_{ht} + (\dot{n}\,\bar{h})_1 = (\dot{n}\,\bar{h})_2 + (\dot{n}\,\bar{h})_3 \tag{16}$$

$$\frac{\dot{Q}_{ht}}{T_h} + (\dot{n}\,\bar{s})_1 + \dot{S}_{gen} = (\dot{n}\,\bar{s})_2 + (\dot{n}\,\bar{s})_3 \tag{17}$$

Using these equations,

$$\dot{Q}_{ht} - \dot{Q}_{ht}\frac{T_o}{T_h} - \dot{S}_{gen}\,T_o = \dot{n}_2(\bar{h} - T_o\bar{s})_2 + \dot{n}_3(\bar{h} - T_o\bar{s})_3 - \dot{n}_1(\bar{h} - T_o\bar{s})_1 \tag{18}$$

$$= \dot{n}_2\,\bar{g}_2 + \dot{n}_3\,\bar{g}_3 - \dot{n}_1\,\bar{g}_1 \tag{19}$$

$$\dot{Q}_{ht} = \frac{\dot{n}_2\,\bar{g}_2 + \dot{n}_3\,\bar{g}_3 - \dot{n}_1\,\bar{g}_1 + \dot{S}_{gen}\,T_o}{1 - \frac{T_o}{T_h}} \tag{20}$$

The least heat of separation is for $\dot{S}_{gen} = 0$,

$$\dot{Q}_{ht,least} = \frac{\dot{n}_2 \bar{g}_2 + \dot{n}_3 \bar{g}_3 - \dot{n}_1 \bar{g}_1}{1 - \frac{T_o}{T_h}} \quad (21)$$

The following conditions are assumed for calculating the least heat and maximum theoretical GOR for HDH:

1. For HDH the recovery ratio is typically <10%. Here for the sake of calculation it is taken as 10%.
2. The inlet feed stream salinity is taken as 35,000 ppm and is approximated by a 0.62 mol/kg NaCl solution.
3. Pressure is 1 bar.
4. Top and bottom temperatures are taken as 90°C and 30°C respectively.
5. The calculation is performed for water production of 1 kg/s.
6. The air stream enters and leaves at the same temperature and humidity. State 4 and 5 in Fig. 19 are the same. $T_{a,out} = T_{a,in}$ and $\omega_{a,out} = \omega_{a,in}$.

At these conditions,

$$\text{GOR} = \frac{h_{fg}}{\left(\frac{\dot{n}_2 \bar{g}_2 + \dot{n}_3 \bar{g}_3 - \dot{n}_1 \bar{g}_1 + \dot{S}_{gen} T_o}{1 - \frac{T_o}{T_h}} \right)}$$

$$= 122.515$$